

UDC 669.15'28-198

DOI: 10.15587/1729-4061.2021.230078

# IDENTIFICATION OF PATTERNS IN THE STRUCTURAL AND PHASE COMPOSITION OF THE DOPING ALLOY DERIVED FROM METALLURGICAL WASTE PROCESSING

*This paper reports a study into the structural-phase composition of the doping alloy made by processing metallurgical anthropogenic waste involving reduction smelting. This is required for determining the technological parameters that ensure an increase in the level of extraction of target elements during the processing of anthropogenic waste and for the further use of the doping alloy. It was revealed that the phase composition of the doping alloy manifested a solid solution of the doping elements and carbon in  $\alpha$ -Fe. Cementite  $Fe_3C$  and silicides  $Fe_5Si_3$ ,  $FeSi$ , and  $FeSi_2$  were also identified. In this case, the doping elements were more likely to act as substitution atoms. It has been determined that the microstructure of the alloy consisted of several phases of different shapes and contents of the basic doping elements. Sites with an elevated iron level of up to 95.87 % by weight in the composition could be represented by the solid solution phase of the doping elements and carbon in  $\alpha$ -Fe. The sites with a relatively high (% by weight) content of carbon (0.83–2.17) and doping elements – W, up to 39.41; Mo, up to 26.17; V, to 31.42; Cr, to 9.15 – were apparently of a carbide nature. The sites with a silicon content of 0.43–0.76 % by weight likely included silicide compounds. The alloy's characteristics make it possible to smelt steel grades without strict carbon restrictions, replacing some of the standard ferroalloys. Neither phases nor compounds with a relatively high propensity for sublimation were identified in the material produced. Therefore, there is no need to provide conditions to prevent evaporation and loss in the gas phase of the doping elements. That could increase the degree of extraction of the doping elements*

**Keywords:** *oxide anthropogenic waste, doped steel scale, reduction smelting, X-ray phase examination*

**Anatolii Poliakov**

PhD, Associate Professor

Department of Machine Repair, Energy Facilities Operation and Labor Protection\*\*

**Anatolii Dzyuba**

PhD, Associate Professor\*

**Vadym Volokh**

PhD, Associate Professor\*

**Artem Petryshchev**

PhD, Associate Professor

Department of Labour and Environment Protection

Zaporizhzhia Polytechnic National University

Zhukovskoho str., 64, Zaporizhzhya, Ukraine, 69063

E-mail: kafedrales@ukr.net

**Bohdan Tsymbal**

PhD

Department of Occupational, Technogenic and Environmental Safety

National University of Civil Defence of Ukraine

Chernyshevska str., 94, Kharkiv, Ukraine, 61023

**Mykhail Yamshinskij**

Doctor of Technical Sciences, Associate Professor\*\*\*

**Ivan Lukianenko**

PhD\*\*\*

**Andrey Andreev**

Doctor of Pedagogical Sciences, Associate Professor, Head of Department

Department of General and Applied Physics

Zaporizhzhia National University

Zhukovskoho str., 66, Zaporizhzhia, Ukraine, 69600

**Tamara Bilko**

PhD, Associate Professor

Department of Occupational Safety and Environmental Engineering

National University of Life and Environmental Sciences of Ukraine

Heroiv Oborony str., 15, Kyiv, Ukraine, 03041

**Victor Rebenko**

PhD, Associate Professor

Department of Mechanization of Animal Husbandry

National University of Life and Environmental Sciences of Ukraine

Heroiv Oborony str., 15, Kyiv, Ukraine, 03041

\*Department of Mechanization of Production Processes in the Agroindustrial Complex\*\*

\*\*Luhansk National Agrarian University

Slobozhanska str., 68, Starobilsk, Ukraine, 92703

\*\*\*Department of Foundry of Ferrous and Nonferrous Metals

National Technical University of Ukraine "Igor Sikorsky Kyiv Polytechnic Institute"

Peremohy ave., 37, Kyiv, Ukraine, 03056

Received date 02.03.2021

Accepted date 15.04.2021

Published date 30.04.2021

**How to Cite:** Poliakov, A., Dzyuba, A., Volokh, V., Petryshchev, A., Tsymbal, B., Yamshinskij, M., Lukianenko, I., Andreev, A., Bilko, T., Rebenko, V. (2021). Identification of the features of the structural and phase composition of the alloying alloy obtained by processing metallurgical waste. *Eastern-European Journal of Enterprise Technologies*, 2 (12 (110)), 38–43. doi: <https://doi.org/10.15587/1729-4061.2021.230078>

## 1. Introduction

Raw materials deposits are getting increasingly depleted every year, which leads to a tendency for the prices of

refractory doping elements to rise in the world market [1]. One way to save resources is to produce doping materials containing molybdenum, tungsten, chromium, vanadium obtained through processing and return to production of

doped anthropogenic waste. Significant amounts of industrial waste doped with refractory elements are not utilized effectively enough in practice. Among such wastes are the oxide and finely-dispersed dust, the scale of tungsten-molybdenum fast-cutting steels. The high doping degree indicates the need to take into consideration the complex nature of the interaction of refractory doping elements when determining the manufacturing parameters of processing. In such waste, the targeted doping elements may be in the form of complex oxide compounds. These circumstances lead to certain issues related to ensuring the manufacturability of the industrial process and the affordable cost of production [2], which is an important condition for making products competitive in the global and domestic markets.

Therefore, it is a relevant task to reduce the loss of doping elements and devise resource-saving technologies in the steel industry during the processing of doped anthropogenic waste. In order to resolve this issue, it is necessary to expand the understanding of the physical and chemical transformations that occur during the reduction smelting of anthropogenic raw materials.

---

## 2. Literature review and problem statement

---

Based on the study results reported in [3], the iron scale consists of  $\text{Fe}_3\text{O}_4$ ,  $\text{Fe}_2\text{O}_3$  and  $\text{FeO}$ . The cited work describes a study into the reduction of iron scale at temperatures of 750...1,050 °C. The largest reduction degree was achieved at 1,050 °C at the content of iron of 98.40 % by weight in the reduction products. After different heat treatment regimes,  $\text{Fe}_3\text{C}$  and  $\text{C}$  were identified in the reduction products along with the iron phase. Similar results with the manifestation of  $\text{Fe}_3\text{C}$  were reported in [4]. It considered the reduction of oxide waste of doped steels, containing, among others, chromium and molybdenum, with carbon. In the products of the reduction smelting of doped waste involving carbon and silicon, the authors of paper [5] identified the phase of iron and  $\text{Fe}_3\text{C}$ . The  $\text{Fe}_3\text{C}$  silicide formation also took place in the Fe-Cr-C-Si system in work [6] that investigated a coating made from the 45Fe39Cr6C10Si alloy. Consequently, the reduction of oxide waste of doped steel using silicon can be accompanied by the formation of iron silicides with dissolved doping elements as substitution atoms. The disadvantages include limited information related to studying the physical and chemical properties of reduction products involving elements such as tungsten and vanadium. The unresolved parts of the issue are the identification of the most acceptable parameters for the reduction of doped anthropogenic raw materials in the Fe-W-Mo-C-V-O-C-Si system.

A study into the course of reactions in the W-O-C system, reported in work [7], showed the stages in  $\text{WO}_3$  reduction through the formation of  $\text{WO}_x$ -type oxides yielding W. Similar transformation stages were observed by the authors of paper [8] when the process temperature rose from 750 °C to 900 °C. Further step-by-step temperature increase to 1,450 °C ensured a predominance of tungsten carbides in the reaction products. The authors of work [9] confirmed, when studying reactions in the Mo-O-C system, the progress of the primary conversion of  $\text{MoO}_3$  to  $\text{MoO}_2$ , which has a lower propensity for sublimation. At the same time, it is not possible to trace the impact exerted on the reduction process by other elements that are present in the doped anthropogenic raw materials. Work [10] also identified the for-

mation of  $\text{MoO}_2$  as an intermediate reduction product that later passed to Mo and carbides. Consequently, the Mo-O-C system, as well as W-O-C, demonstrates the stages of transformation but it is not possible to trace the features of the reduction involving the complex participation of doping elements. The downside is that the form of tungsten- and molybdenum-containing compounds present in highly-doped steel oxides can be more difficult, different from individual pure oxides. The unresolved parts of the issue relate to determining the technological parameters for the reduction of oxide anthropogenic complexly-doped raw materials with the yield of material that does not contain sublimation-prone phases and compounds. That could make it possible to eliminate the need to create additional conditions to prevent the loss of target elements with the gas phase.

The possibility of parallel reduction and formation of  $\text{Cr}_{23}\text{C}_6$ ,  $\text{Cr}_3\text{C}_2$  and  $\text{Cr}_7\text{C}_3$  in the temperature interval of 1,273–1,773 K in the Fe-Cr-O-C system is considered by the authors of work [11]. Paper [12] investigated the reduction of  $\text{FeO}\cdot\text{V}_2\text{O}_3$  and  $\text{FeO}\cdot\text{Cr}_2\text{O}_3$  oxides at 1,100–1,250 °C. When C:Fe in the charge changes from 0.8 to 1.4, an increase in the extraction of V and Cr (%) was detected from 10.0 to 45.3, and from 9.6 to 74.3, respectively. Processing at 1,250 °C led to an increase in the formation of carbides. The disadvantage is the lack of data on the reduction of complex oxides, which may occur in the composition of anthropogenic raw materials, which can lead to some differences in the process of reaction. The unresolved parts of issue relate to broadening the perception of the nature of the presence of elements in reduction products involving the integrated use of raster electron microscopy, X-ray microanalysis, and X-ray phase analysis.

One should note the results of studying the carbon-thermal treatment of anthropogenic waste of unalloyed steels reported in work [3], which identified the phases of iron, carbide of iron, and carbon in the reduced material. Similar data were acquired by the authors of papers [4, 5] when studying the reduction of doped anthropogenic waste with carbon and silicon. The reduced material revealed a phase of iron with dissolved doping elements, as well as silicides and iron carbides. The formation of iron silicide was also noted by the authors of paper [6] when studying the interaction of elements in the Fe-Cr-C-Si system. Reduction studies in the W-O-C [7, 8] and Mo-O-C [9, 10] systems have shown the stages of transformation through the formation of intermediate oxides, followed by the metal and carbide phases. In reduction studies, the Fe-Cr-O-C and Fe-V-O-C systems [11, 12] demonstrated the carbide-forming processes along with reduction. At the same time, some excess of the reducer was needed to increase the degree of extraction of the target elements. However, defining the features in the phase composition and microstructure of the carbon- and silicon- reduced complexly doped W, Mo, Cr, V anthropogenic raw materials is unresolved. At the same time, the use of raster electron microscopy, X-ray microanalysis, and X-ray phase analysis would improve the understanding of the nature of the presence of components in the reduced material. It is advisable to carry out research on the features of phase and structural compositions of the doping alloy derived from anthropogenic waste involving carbon and silicon. It is also necessary to define the technological parameters of reduction to obtain the material without phases and compounds that have a propensity

for sublimation. That could reduce the loss of doping elements by sublimating oxide compounds and phases when receiving and using a reduced doping material.

### 3. The aim and objectives of the study

The purpose of this work was to identify the features of structural-phase transformations in the processing of metallurgical oxide anthropogenic waste, doped with W, Mo, Cr, V, in order to yield a doping alloy. This is necessary to increase the extraction degree of doping elements during the processing of oxide anthropogenic raw materials and to the further use of the alloy during doping.

To accomplish the aim, the following tasks have been set:

- to determine the phase composition of an alloy derived from doped anthropogenic waste regarding the nature of the presence of elements;
- to investigate the microstructure and chemical composition of individual phase alloy formations derived from doped anthropogenic waste, involving the complex use of raster electron microscopy and X-ray microanalysis.

### 4. Materials and methods to study the properties of an alloy

#### 4.1. The materials and equipment used in the experiment

The starting raw material is the scale of tungsten-molybdenum-containing grades of fast-cutting steel, formed at the sites of metallurgical production. The reducer is ultrafine carbon dust derived from coal-graphite production; its addition provided for a mass ratio of O:C in the charge at 1.33. The additional oxidizing capacity of the alloy was achieved by the addition of FS-65 ferrosilicon to the charge with a mass ratio of Si:C in the charge at 0.19. The addition of the shavings of force grinding of fast-cutting steels to the charge ensured the intensification of heat exchange in the initial stages of heating. Samples for our research were smelted in alundum crucibles in an indirect heating furnace with a coal lining. The smelting temperature was 1,873–1,913 K. After smelting, the alundum crucibles were removed from the furnace with the alloy and cooled at the ambient air temperature.

X-ray phase analysis of the samples was performed at the diffractometer “DRON-6” (Russia).

Images of the microstructure and the chemical composition of individual parts of the surface of the samples were acquired from the “JSM 6360LA” raster electron microscope, equipped with the JED 2200 X-ray microanalysis system manufactured by JEOL (Japan).

#### 4.2. Procedure to determine the indicators of samples properties

The phase composition of the samples was determined by X-ray phase analysis. Monochromatic radiation of Cu K $\alpha$  was used at  $\lambda=1.54051 \text{ \AA}$ . The tube voltage and the anode current were 40 kV and 20 mA, respectively. The composition of the phases was determined using the PDWin 2.0 software (Russia).

Microstructure images were acquired at an accelerating voltage of 15 kV. The diameter of the electronic probe was 4 nm. The percentage of chemical elements was determined by a reference-free method of calculating fundamental parameters.

### 5. Results of studying the properties of the doping alloy

#### 5.1. Determining the characteristics of the phase composition of the doping alloy

Our study of the composition of the doping alloy has established the presence of several phases (Fig. 1).

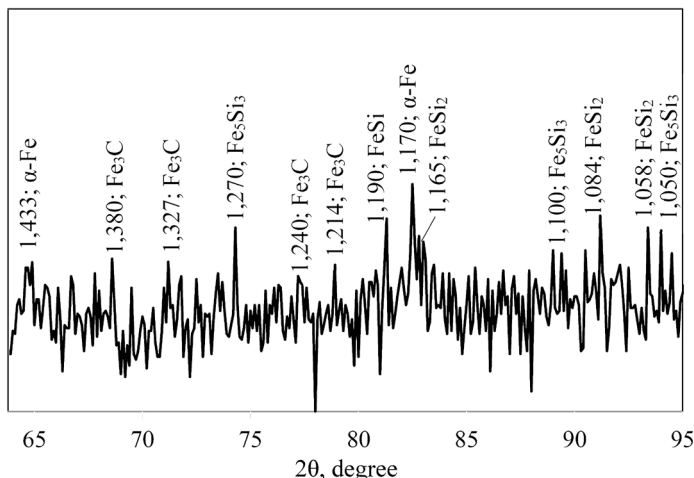


Fig. 1. X-ray phase examination of the doping alloy

The manifestation of the phase of solid carbon solution and doping elements in the  $\alpha$ -Fe was revealed. The carbide component was represented by  $\text{Fe}_3\text{C}$ . At the same time, the composition revealed the silicides of iron  $\text{Fe}_5\text{Si}_3$ ,  $\text{FeSi}$ , and  $\text{FeSi}_2$ . Individual compounds of doping elements throughout the scanning interval were shown fragmentally with a relatively low intensity of diffraction highs, which were approaching the background level.

#### 5.2. Studying the microstructure of the doping alloy

In the alloy studied, the microstructure consisted of several phases of different shapes and compositions (Fig. 2, 3, Table 1).

Table 1

The results of X-ray microanalysis of the doping alloy corresponding to Fig. 2

Examined sites	Element content, % by weight							Total
	C	Si	V	Cr	Fe	Mo	W	
1	2.17	0.00	30.75	7.28	16.51	15.91	27.38	100.00
2	0.95	0.00	5.82	7.93	19.72	26.17	39.41	100.00
3	0.83	0.00	5.64	7.72	20.88	25.89	39.04	100.00
4	0.12	0.49	0.00	2.46	95.87	1.06	0.00	100.00
5	0.08	0.43	0.00	2.61	95.60	1.28	0.00	100.00
6	1.73	0.64	2.20	8.82	79.61	2.71	4.29	100.00
7	2.09	0.00	31.42	7.42	16.59	15.55	26.93	100.00
8	1.61	0.76	2.06	9.15	79.41	2.53	4.48	100.00

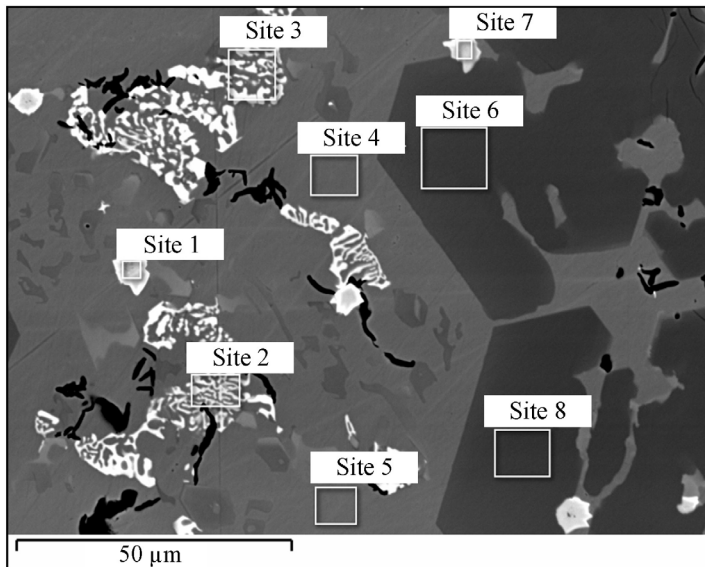


Fig. 2. Image of the microstructure of the doping alloy at magnification  $\times 1,000$ : 1–8 – sites of X-ray microanalysis

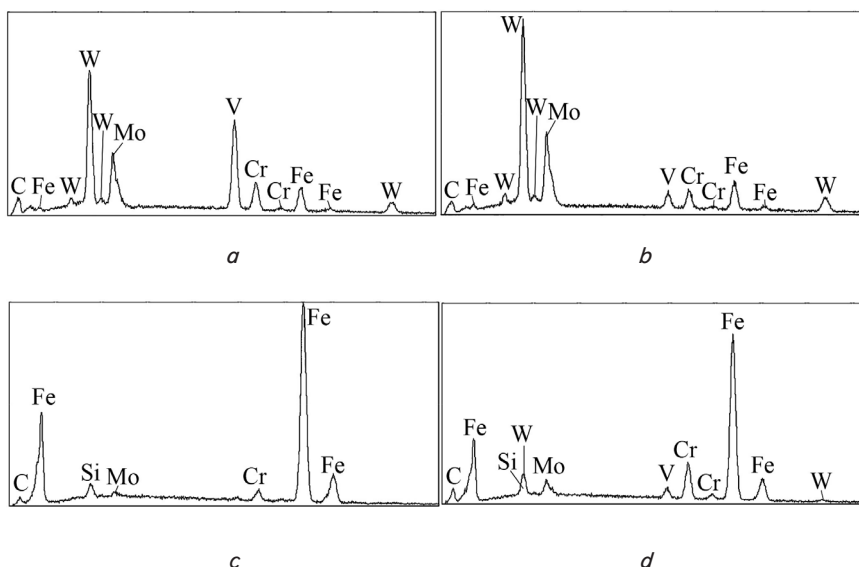


Fig. 3. Spectrograms of the X-ray microanalysis of some examined sites of the resulting alloy corresponding to Fig. 2: a – 1; b – 3; c – 4; d – 8

The sites with a relatively high content of W and Mo were identified (Fig. 2, sites 2, 3, Table 1) where the level of elements amounted to 39.41 % by weight and to 26.17 % by weight, respectively. The Cr content at the examined sites ranged from 2.46 to 9.15 % by weight. Phases with a V content corresponded to sites 1–3 and 6–8. At the same time, at the examined sites 1 and 7 the content of V reached 31.42 % by weight. The presence of Si was found at sites 4–6 and 8 at 0.43–0.76 % by weight. Carbon manifested itself at all the sites studied, in the amount of 0.08–2.17 % by weight. There was a clear separation of phases with the difference in the content of the elements. One can see the presence of different phases with relatively low and high Fe content (Fig. 2, sites 4, 5, 6, 8). The change in Cr's content in these phases was reversed relative to Fe. The doping elements demonstrated a higher concentration in the inclusions that formed the mesh-

like structure (Fig. 2, sites 2, 3). The inclusions with a relatively high V content were rounded (Fig. 2, sites 1, 7). The examined sites with higher levels of doping elements, however, demonstrated a relatively high carbon concentration (Fig. 2, sites 1–3, 6–8).

## 6. Discussion of results of studying the properties of the doping alloy

Our study of the phase composition of the alloy (Fig. 1) has shown the principle of the existence of doping elements in the lattice  $\alpha$ -Fe in the form of a solid solution. This feature is consistent with the results reported in [4]. Some of the doping elements as substitution atoms may be present in carbide and silicide compounds, which is consistent with the data from [5, 6]. However, the authors of the cited works did not reveal the presence of  $\text{Fe}_5\text{Si}_3$  silicide in the samples examined. And, in work [5], the samples included the silicide  $\text{Fe}_3\text{C}$ , which is different from our study. Based on the diffractogram reported in the current paper, some of the identified diffraction highs demonstrated intensity not much higher than the background level. Identification of such peaks was carried out as an addition, along with the relatively intense diffraction highs detected. The presence of some unsigned peaks relates to those compounds whose manifestation was weakly expressed and fragmented in character.

The comprehensive study into the features of microstructure using X-ray microanalysis of the alloy additionally shows the concentration of doping elements in the carbide and silicide components, as well as in the form of a solid solution in the lattice  $\alpha$ -Fe (Fig. 2, 3, Table 1). At the same time, some of the sites studied were relatively high in chromium and carbon, as well as demonstrated the presence of silicon (Fig. 2, sites 6, 8). This may indicate local regions with the presence of iron-chromium-containing carbides or silicides, which is consistent with the results reported in [11]. The authors of that work demonstrated the possibility of a parallel course of the reduction and carbide-forming processes.

The results from an X-ray microanalysis study indicate that the resulting alloy likely refers to a high-carbon type. This is due to that most sites in the sample studied were characterized by carbon content at the level of hypereutectoid steel (Fig. 2, Table 1, sites 2, 3, 6–8; from 0.83 to 2.09 % by weight). The high-carbon type of the alloy is also further indicated by the results from X-ray phase examinations with a relatively intense manifestation of the carbide component (Fig. 1).

Identification of a solid solution of the doping elements, as well as carbon in the lattice  $\alpha$ -Fe (Fig. 1), is predetermined by the presence of the ferrite phase, which is in the mixture with the cementite phase. The mixture of ferritic and cementite phases can be characteristic, among other

things, of alloys with relatively high carbon content (at the level of hypereutectoid steel).

The microstructure regions with relatively high levels of W, Mo, V, and carbon (Fig. 2, sites 1–3, 7) appear to be carbide compounds. This is consistent with the results reported in works that describe the propensity for carbide formation during the carbon-thermal treatment of W – [8], Mo – [9, 10], and V – [12]. At the same time, inclusions with a relatively high vanadium content (Fig. 2, sites 1, 7) had differences in shape and contours, compared to phases characterized by the increased levels of other refractory elements. That leads to the possibility of the presence of at least two variations of carbide phases with refractory elements. At the same time, the differences in the results reported here are in the presence at the studied sites of the alloy based on the reduced anthropogenic waste from the complex of iron and several refractory elements. This may indicate a more complex nature of compounds. A different composition of the doping elements can indicate the different nature of the formed particles.

The lack of images of the microstructure with the distribution of the main elements in the characteristic X-rays at the examined surface of the alloy is a limitation of the study. That could have provided for better visibility in the representation of the features of the microstructure and the nature of the presence of doping elements.

The vector to advance this area is directed towards the use for processing, by reduction smelting, the doped waste from the production of other classes of steel and alloys. It is also advisable to further study the patterns in the physical and chemical properties of the doping alloy when changing the ratio of the oxidizer and reducer in the charge in order to determine the most acceptable technological aspects. The difficulty in trying to expand the current study relates to that the experimental base was not sufficient.

Certain restrictions in the use of the alloy may be associated with complex doping. This is due to the need to choose for doping the target classes of steels close in the content of the basic elements. Problems may occur if one or more alloy components are strictly limited in the target product and can result in exceeding the set limits of the elements in the composition. To prevent these kinds of problems, and to ensure relatively high consumption rates, it is required that

the composition of the elements in the alloy and the target product should be close. The alloy's characteristics allow steel grades to be smelted without strict carbon restrictions, replacing some of the standard ferroalloys. From this perspective, the fast-cutting steel grades R6M5, R6M5F3, R12M3K5F2, and others, are promising as their smelting involves an electric arc furnace. The absence of phases and compounds with an increased propensity for sublimation in the resulting material does not require additional conditions to prevent evaporation and loss of doping elements into the gas phase. This leads to an increase in the degree of extraction of doping elements. When the alloy is produced, anthropogenic waste is reduced with the presence of doping elements in the solid solution in the crystal lattice of the iron phase, as well as in the composition of carbides and silicides. Residual carbon and silicon manifested themselves in the form of carbide and silicide phases, providing the necessary reducing and oxidizing capacities when using the alloy. At the same time, the processing and return to the production of metallurgical anthropogenic waste ensures a reduction in pollution and improved environmental safety of the industrialized regions.

---

## 7. Conclusions

---

1. It has been revealed that the phase composition of the doping alloy demonstrated the manifestation of a solid solution of carbon and doping elements in the lattice  $\alpha$ -Fe. Fe<sub>3</sub>C cementite and Fe<sub>5</sub>Si<sub>3</sub>, FeSi, and FeSi<sub>2</sub> silicides were also identified. In this case, the doping elements were more likely to act as substitution atoms.

2. It has been determined that the microstructure of the alloy consisted of several phases of different shapes and contents of doping elements. The sites with an elevated iron level of up to 95.87 % by weight could be represented by a solid solution of carbon and doping elements in the lattice  $\alpha$ -Fe. The sites with a relatively high carbon content (% by weight) of 0.83–2.17, and the doping elements – W, up to 39.41; Mo, up to 26.17; V, to 31.42; Cr, to 9.15, apparently had a carbide nature. The sites with silicon in the composition at the level of 0.43–0.76 % by weight could include silicide compounds.

---

## References

1. Henckens, M. L. C. M., van Ierland, E. C., Driessen, P. P. J., Worrell, E. (2016). Mineral resources: Geological scarcity, market price trends, and future generations. *Resources Policy*, 49, 102–111. doi: <https://doi.org/10.1016/j.resourpol.2016.04.012>
2. Sekiguchi, N. (2017). Trade specialisation patterns in major steelmaking economies: the role of advanced economies and the implications for rapid growth in emerging market and developing economies in the global steel market. *Mineral Economics*, 30 (3), 207–227. doi: <https://doi.org/10.1007/s13563-017-0110-2>
3. Mechachti, S., Benchiheb, O., Serrai, S., Shalabi, M. (2013). Preparation of iron Powders by Reduction of Rolling Mill Scale. *International Journal of Scientific & Engineering Research*, 4 (5), 1467–1472.
4. Petryshchev, A., Milko, D., Borysov, V., Tsybmal, B., Hevko, I., Borysova, S., Semenchuk, A. (2019). Studying the physicalchemical transformations at resourcesaving reduction melting of chrome–nickelcontaining metallurgical waste. *Eastern-European Journal of Enterprise Technologies*, 2 (12 (98)), 59–64. doi: <https://doi.org/10.15587/1729-4061.2019.160755>
5. Petryshchev, A., Braginec, N., Borysov, V., Bratishko, V., Torubara, O., Tsybmal, B. et. al. (2019). Study into the structuralphase transformations accompanying the resourcesaving technology of metallurgical waste processing. *Eastern-European Journal of Enterprise Technologies*, 4 (12 (100)), 37–42. doi: <https://doi.org/10.15587/1729-4061.2019.175914>
6. Azimi, G., Shamanian, M. (2010). Effects of silicon content on the microstructure and corrosion behavior of Fe–Cr–C hardfacing alloys. *Journal of Alloys and Compounds*, 505 (2), 598–603. doi: <https://doi.org/10.1016/j.jallcom.2010.06.084>

7. Baghdasaryan, A. M., Niazyan, O. M., Khachatryan, H. L., Kharatyan, S. L. (2014). DTA/TG study of tungsten oxide and ammonium tungstate reduction by (Mg+C) combined reducers at non-isothermal conditions. *International Journal of Refractory Metals and Hard Materials*, 43, 216–221. doi: <https://doi.org/10.1016/j.ijrmhm.2013.12.003>
8. Islam, M., Martinez-Duarte, R. (2017). A sustainable approach for tungsten carbide synthesis using renewable biopolymers. *Ceramics International*, 43 (13), 10546–10553. doi: <https://doi.org/10.1016/j.ceramint.2017.05.118>
9. Torabi, O., Golabgir, M. H., Tajizadegan, H., Torabi, H. (2014). A study on mechanochemical behavior of MoO<sub>3</sub>–Mg–C to synthesize molybdenum carbide. *International Journal of Refractory Metals and Hard Materials*, 47, 18–24. doi: <https://doi.org/10.1016/j.ijrmhm.2014.06.001>
10. Zhu, H., Li, Z., Yang, H., Luo, L. (2013). Carbothermic Reduction of MoO<sub>3</sub> for Direct Alloying Process. *Journal of Iron and Steel Research International*, 20 (10), 51–56. doi: [https://doi.org/10.1016/s1006-706x\(13\)60176-4](https://doi.org/10.1016/s1006-706x(13)60176-4)
11. Simonov, V. K., Grishin, A. M. (2013). Thermodynamic analysis and the mechanism of the solid-phase reduction of Cr<sub>2</sub>O<sub>3</sub> with carbon: Part 1. *Russian Metallurgy (Metally)*, 2013 (6), 425–429. doi: <https://doi.org/10.1134/s0036029513060153>
12. Zhao, L., Wang, L., Chen, D., Zhao, H., Liu, Y., Qi, T. (2015). Behaviors of vanadium and chromium in coal-based direct reduction of high-chromium vanadium-bearing titanomagnetite concentrates followed by magnetic separation. *Transactions of Nonferrous Metals Society of China*, 25 (4), 1325–1333. doi: [https://doi.org/10.1016/s1003-6326\(15\)63731-1](https://doi.org/10.1016/s1003-6326(15)63731-1)